Seismic detection of fluid saturation in aligned fractures

Enru Liu and Xiang-Yang Li, Edinburgh Anisotropy Project, British Geological Survey*

Summary

The application of fracture-induced anisotropy has evolved from the estimation of fracture orientation and intensity to the prediction of fluid saturation and permeability anisotropy in fractured reservoirs. For this, we examine the sensitivity of fracture compliance to fluids, and derive simple analytical expressions which link seismic anisotropic measurements to pore or fracture fluids. We show that the normal to shear compliance ratio is directly related to fluid saturation, and to the P- and S-wave reflectivities and the effective Thomsen (1986) anisotropic parameters, and thus can be estimated from seismic data. Existing laboratory and field data are used to verify the results.

Introduction

The study of azimuthal anisotropy provides a way of detecting the aggregate alignments, intensity and distribution of sub-seismic fractures and pores, which control much of the mechanical strength and transport properties of the rock structure. Over recent years, interest in this subject has evolved from the estimation of stress/fracture orientation, prediction of spatial variation of fracture intensity, to the estimation of fluid flow, permeability anisotropy and pressure prediction in reservoirs. In this paper the analytic fracture models studied by Hudson and Liu (1999) and Liu et al. (2000) are used to study the effects of pore or fracture filling fluids. We derive simple analytical expressions which link the fracture compliances to pore fluids, and to fracture-induced P- and S-wave anisotropic measurements characterized by the effective Thomsen (1986) parameters. By analysis of existing laboratory and field data, we show that the ratio of normal to shear compliances and the ratio of the P- to S-wave fractured anisotropy can be used as effective fluid indicators.

Modelling a fracture

In modelling the seismic response of natural fractures, it is essential to understand the microscopic details of fractures as fluid flow is controlled by micro-structures of fracture or fault planes. Intensive studies have addressed this problem because of its conceptual and practical importance. The general understanding is that a fracture is a cluster of small cracks, and a fault is a cluster of fractures. Cracks often exist as clusters at different scales. Hudson and Liu (1999) and Liu et al. (2000) suggested that published fracture models can be broadly classified into three groups: (1) a plane distribution of small cracks, (2) a plane distribution of contacts, and (3) a thin layer of a constant aperture with the appropriate material infill, as shown in Figure 1. All three types of fractures can be mathematically represented as a planar boundary across which the stresses are continuous, whereas the displacements are discontinuous.

The simplest model is the so-called slip interface model, as proposed by Schoenberg (1980), Pyrak-Nolte et al. (1990), and others, i.e.

$$[\boldsymbol{u}] = \boldsymbol{Zt}, \tag{1}$$

where $[\boldsymbol{u}]$ is the average displacement discontinuity on the fracture and $\boldsymbol{t}$ is the traction on the fracture. The tensor $\boldsymbol{Z}$ is usually diagonal, i.e. $\boldsymbol{Z} = \mathrm{diag}\{Z_T, Z_T, Z_N\}$.

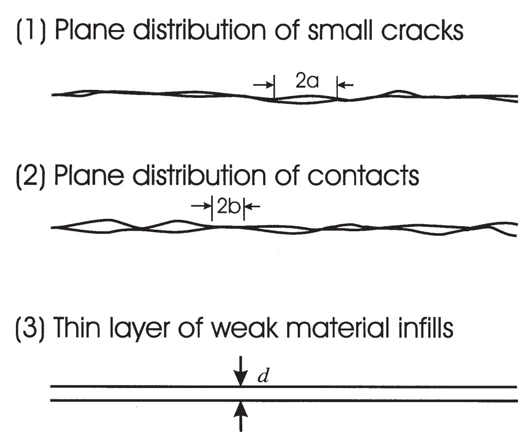

Figure 1. Three fracture models. (1) A plane distribution of small cracks; (2) a plane distribution of contacts, and (c) a thin layer of weak solid with a constant aperture.

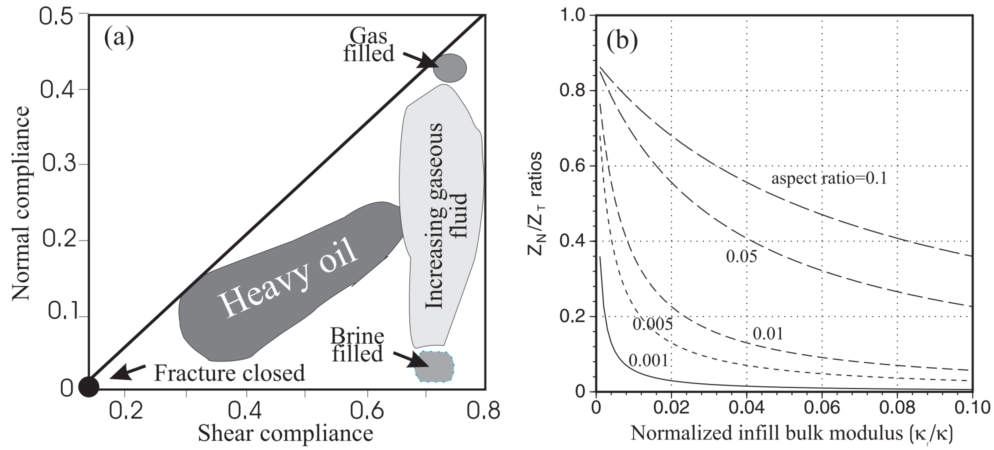

Figure 2. (a) Schematic illustration of sensitivity of normal and shear fracture compliance to fluids. (b) Variation of normal to shear fracture compliance ratio as a function of normalized fracture infill bulk modulus computed for various aspect-ratios of cracks.

Equivalent medium theory

Aligned fractures give rise to transverse isotropy with a horizontal axis of symmetry, which has five elastic constants. If we model fractures as a plane distribution of small cracks, these elastic constants (c_{ij}) may be written as, to the first order of crack density,

$$c_{11} = (\lambda + 2\mu)\left[1 - (\lambda + 2\mu)Z_N\right], \quad (2)$$

$$c_{22} = c_{33} = C_{11} + 4\mu(\lambda + \mu)Z_N \quad (3)$$

$$c_{12} = c_{13} = c_{21} = c_{31} = \lambda\left[1 - (\lambda + 2\mu)Z_N\right], \quad (4)$$

$$C_{23} = C_{32} = C_{12} + 2\lambda\mu Z_N, \quad (5)$$

$$C_{55} = C_{66} = \mu(1 - \mu Z_T), \quad (6)$$

where

$$Z_N = \frac{\epsilon_d U_{33}}{\mu}, \quad Z_T = \frac{\epsilon_d U_{11}}{\mu}, \quad (7)$$

λ and μ are the Lamé constants of the background medium, ϵ_d is the crack density, and U_{11} and U_{33} are the response of a single crack to shear traction and tension, respectively (Hudson and Liu 1999).

Z_N/Z_T as an indicator of fracture fluids

An indicator of fluid content in fractures proposed by Schoenberg (1998) is the normal to shear compliance ratio (Z_N/Z_T). For example, if fractures are dry, $Z_N/Z_T \simeq 1$, and if fractures are filled with liquid, $Z_N/Z_T \simeq 0$. In general, the ratio of normal to shear compliances is dependent on the fracture interior boundary conditions, in particular the fluid types as schematically shown in Figure 2a. For simplicity, we assume that the shear modulus of fluids is zero and that the matrix rock is a Poisson medium. For a distribution of isolated or interconnected cracks clustering on a surface, the compliance ratio is given by

$$\frac{Z_N}{Z_T} = \frac{7}{8}\left[1 + \frac{5}{2\pi}\left(\frac{a_c}{c_c}\right)\left(\frac{\kappa_f}{\kappa}\right)\right]^{-1}, \quad (8)$$

where a_c and c_c are the long and short axes of the elemental cracks on the fracture planes (c_c/a_c is called the aspect ratio and is assumed to be small), κ_f and κ are the bulk moduli of fluids and matrix, respectively.

Figure 2b shows the variations of the fracture compliance ratio (Z_N/Z_T) with normalized bulk modulus of the fracture infill [κ_f/κ]. The variations were computed for different crack aspect ratios. This figure shows that Z_N/Z_T decreases as bulk modulus of the fracture infill increases, and the rapid change occurs when the fracture infill bulk modulus approaches zero (i.e. gas-filled fractures). This implies that the ability to discriminate fluid types using Z_N and Z_T decreases with aspect ratio. Nevertheless, The quantitative relationship given in equation (8) indicates that Z_N/Z_T can be effectively used as a measure of fluid content in fractures.

Links to P and S-wave reflectivities

Interestingly, using the reflection/transmission coefficients derived by Pyrak-Nolte et al. (1990) for a single fracture, it is easy to show that at low frequency the ratio of the reflection coefficients of P- and S-waves at normal incidence (denoted by R_P and R_S, respectively) is proportional to the fracture compliance ratio,

$$R_P/R_S = Z_N/Z_T\,(\alpha/\beta)\,, \tag{9}$$

where α and β are P- and S-wave velocities of the unfractured rock. Equation (9) indicates that the P and S-wave reflectivities are directly link to the fracture compliance ratio, and may serve as good indicators of fluid saturation.

Links to Thomsen's parameters

Using the equivalent medium theory of fractured rocks, we can also derive

$$\frac{Z_N}{Z_T} = \frac{1}{2(1-\beta/\alpha)^2}\left(\frac{\varepsilon}{\gamma}\right), \tag{10}$$

where ε and γ are the effective Thomsen's anisotropic parameters defined as $\varepsilon = (c_{33} - c_{11})/2c_{11}$ and $\gamma = (c_{44} - c_{66})/2c_{66}$ for fractured rock. c_{ij} are effective elastic constants of the fractured rock given in equations (2) to (6). Since ε and γ show respectively the degrees of P- and shear-wave anisotropy, equation (10) therefore provides a direct link between fluid types and P- and S-wave anisotropy.

Analysis of experimental data

To verify these relationships, we apply the findings to four experimental datasets taken from the literatures. Firstly, we examine the sensitivity of the compliance ratio Z_N/Z_T to fluid saturation. The data are taken from Pyrak-Nolte et al. (1990) and Hsu and Shoenberg (1993). As shown in Figure 3, there is a clear separation between the Z_N/Z_T curves for dry and saturated samples (Figure 3a), and for samples with different honey saturation (Figure 3b). This confirms that the ratios of Z_N/Z_T are very sensitive to the properties of the fracture infill, as predicted by equation (8) and Figure 2.

Secondly, we examine the sensitivity of the anisotropic parameters to fluid saturation. We use elastic constants of reservoir rocks published by Thomsen (1986) and Vernik and Liu (1997). These laboratory data were compiled from a large number of oilfield and a variety of rock samples. As shown in Figures 4a and 4b, we can see clearly that in the cross-plotting of ε and γ, the data are well-separated into two regions corresponding to the dry and saturated samples, in particular for the more recent data of Vernik and Liu (1997). This figure confirms the potential to discriminate fluid types in fractured porous rocks using $P-$ and $S-$wave anisotropic measurements.

Conclusions

We have used the analytic expressions of the fracture compliance $\boldsymbol{Z}$ to study the sensitivity of fracture compliance ratios to fluids. The fracture compliances may be regarded as macroscopic parameters, which can not be determined directly by experiments. However, we show that the normal to shear compliance ratio is directly related to pore or fracture fluids, and to the P- and S wave reflectivities and the Thomsen's anisotropic parameters, and thus can be estimated from seismic data. In general, the assumption of $Z_N/Z_T \simeq 1$ holds for dry fractures, and for liquid-filled fractures, $Z_N/Z_T \simeq 0$. So the Z_N/Z_T ratio can therefore be used as an effective indicator of pore or fracture fluids. Various published field and laboratory data have provided a strong support to this conclusion.

Acknowledgements

This research was supported by a NERC micro-to-Macro grant and the sponsors of the Edinburgh Anisotropy Project, and the paper is published with the approval of the Director of BGS and EAP sponsors: Agip, Amerada Hess, BP Amoco, Chevron, Conoco, Elf, Landmark, Mobil, PGS, Phillips, Saga Petroleum, Schlumberger, Shell, Texaco, TotalFina and Veritas DGC.

References

Hsu, C.H., and Schoenberg, M., 1993, Elastic waves through a simulated fractured medium: Geophysics, **58**, 964-977.

Hudson, J.A., and Liu, E., 1999, Effective elastic properties of heavily faulted structures: Geophysics, **64**, 479-485.

Hudson, J. A., Liu, E., and Crampin, S., 1996, The mechanical properties of materials with interconnected cracks and pores: Geophys. J. Int., **124**, 105-112.

Liu, E., Hudson, J.A., and Pointer, T., 2000, Equivalent medium representation of fractured rock: J. Geophys. Res., in press.

Pyrak-Nolte, L.J., Myer, L.R., and Cook, N.G.W., 1990, Transmission of seismic waves across single natural fractures: J. Geophys. Res., **95**, 8617-8638, 1990.

Schoenberg, M., 1980, Elastic wave behaviour across linear slip interfaces: J. Acoust. Soc. Am., **68**, 1516-1521.

Schoenberg, M., 1998, Acoustic characterization of underground fractures: Expanded Abstract, 68th Ann. Int. SEG Meeting, New Orleans, 1624-1627.

Thomsen, L., 1986, Weak elastic anisotropy: Geophysics, **51**, 1954-1966.

Vernik, L. and Liu, X., 1997, Velocity anisotropy in shales: A petrophysical study: Geophysics, **62**, 521-532.

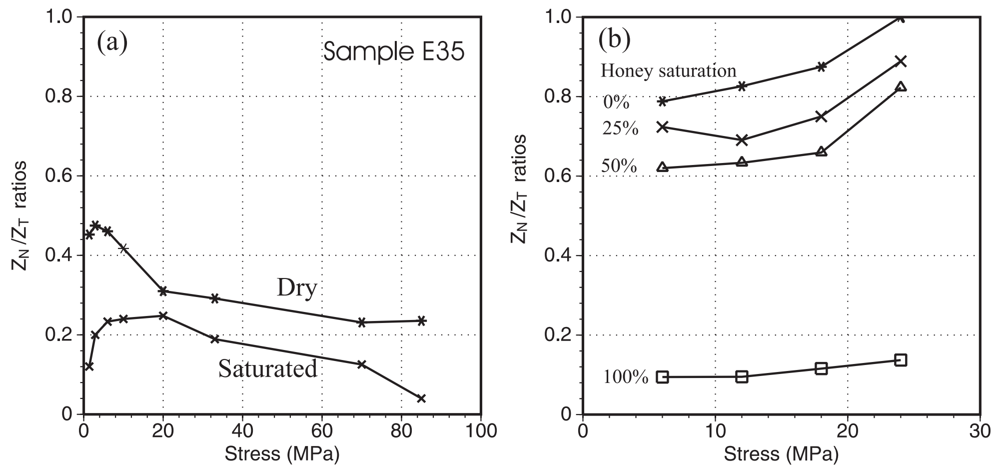

Figure 3. Laboratory data analysis - fracture compliance ratio as a function of stress for different saturation. (a) data are taken from Pyrak-Nolte et al. (1990), and (b) data are taken from Hsu and Schoenberg (1993).

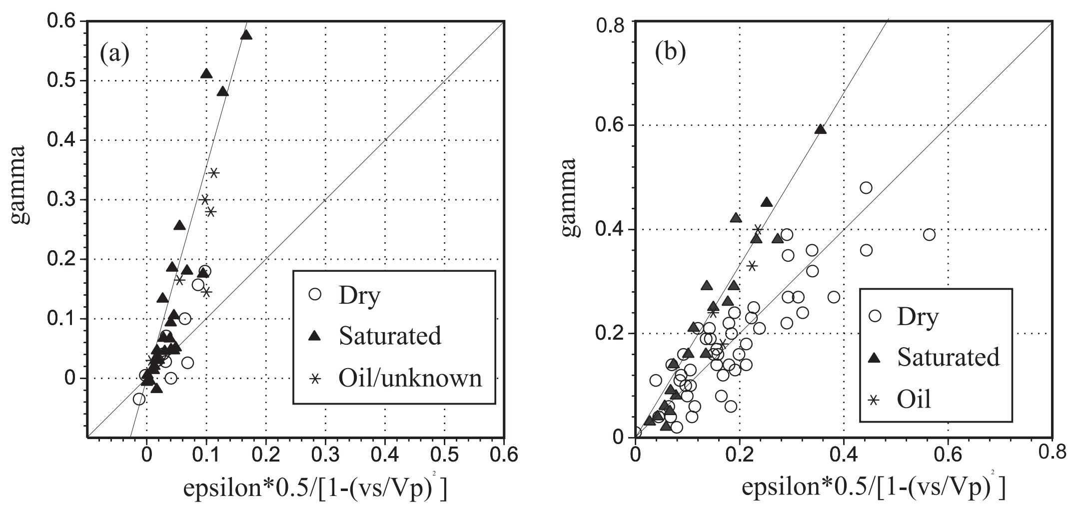

Figure 4. Cross-plots of Thomsen's parameters γ with ε [see equation (2)]. The two lines in each graph are the linear fit to the saturated (solid triangles) and dry samples (open circles). (a) data are taken from Thomsen (1986), and (b) data are taken from Vernik and Liu (1997).